Journal of Applied Polymer Science

Influence of Combined Pretreatment of Quadrol and Anhydrous Ionic Liquid Microemulsion on the Physicochemical Property of Masson Pine

Long Li, Ren-dang Yang, De-tao Liu, Fei Yang
State Key Laboratory of Pulp and Paper Engineering, South China University of Technology, Guangzhou 510640, Guangdong, China
Correspondence to: D.-t. Liu (E-mail: dtliu@scut.edu.cn)

ABSTRACT: The physical properties of laboratory-prepared anhydrous ionic liquid microemulsion, including quasi-ternary phase diagram, conductivity, surface tension, and simulating graph of a microscopic particle system were investigated to maintain the optimum ratio of CTAB (Hexadecyl trimethyl ammonium Bromide) and *n*-butyl alcohol at 1/24 to 1/12. The microemulsion region can reach a maximum of 75% at lower temperatures. We constructed a combined pretreatment of quadrol and anhydrous ionic liquid microemulsion on masson pine powder and analyzed its properties by Fourier-transform infrared, thermogravimetric analysis-derivative thermogravimetry, XRD (X-ray diffraction), and scanning electron microscope. Results showed that hemicellulose and a noncrystalline region in cellulose were disrupted effectively after pretreatment. Relative crystallinity increased from 35.8 to 49.8. A few crystalline structures of cellulose I were recrystallized and then transformed to cellulose II as indicated by IR, XRD, and DTG results. Thermostability decreased, and the region with a main thermal weight loss at 375°C shifted to the region with a lower temperature at 310°C. The yield of glucose can reach to 78.2%, which is 2.2 times than that of untreated powder; the combined pretreatment is an effective method to promote the development of bio-energy. © 2013 Wiley Periodicals, Inc. J. Appl. Polym. Sci. **2014**, *131*, 39794.

KEYWORDS: fibers; biomaterials; structure–property relations; surfaces and interfaces

Received 10 May 2013; accepted 26 July 2013
DOI: 10.1002/app.39794

INTRODUCTION

Lignocellulosic biomass can be used as a low cost and renewable feedstock in bioconversion to produce fermentable sugars, which can be further utilized in biofuel production.[1,2] Approximately more than one billion tons of biomass is available and can be converted to biofuels as a renewable source to reduce a substantial portion of fossil fuels currently consumed in transportation.[3] For instance, woody biomass (hardwoods and softwoods) is a very important feedstock used in cellulosic ethanol production; approximately 370 million tons of oven-dried woody biomass, accounting for 30% of the estimated total biomass available for biofuel production, can be produced annually in the United States.[4] and in other countries such as New Zealand, Canada, and Scandinavia. Thus, wood biomass is possibly an important part of biomass supply that improves bioeconomy if biodiversity, sustainable and healthy forests, and appropriate ecosystem management are promoted to meet local and regional bioenergy needs.

One of the major challenges of the use of lignocellulosic biomass as a source of biofuel production involves the difficulty in cellulose hydrolysis because lignocellulose is covered by a robust and complex structure containing lignin and hemicelluloses, thereby inhibiting the functions of cellulosic enzymes.[5,6] Native cellulose also has high crystallinity arising from intermolecular and intramolecular hydrogen bonding; thus, this material is insoluble in different solvents and hydrolyzation is difficult to establish.[7,8] A compact native structure also prevents chemicals to permeate cellulose; for this reason, a passageway should be opened and accessibility should be initially increased. Although pretreatment is one of the most costly steps in this biochemical process,[9] pretreatment is one of the most important processes in bioenergy production.

Several physical and chemical pretreatment methods are currently used to overcome lignocellulose recalcitrance, increase enzyme efficiency, and improve monomeric sugar yield. These methods include steam explosion,[10] biological reactions,[11] ammonia fiber explosion,[12] dilute acid,[13,14] and alkali treatments.[15] However, such pretreatment processes require higher energy and entail high costs associated with disposal recovery.[16]

The use of ionic liquid (IL) has provided significant application in cellulosic biomass pretreatments.[17] Uju and his group used two ILs of [Emim][OAc] (1-ethyl-3-methylimidazolium acetate) and [Bmpy][Cl] (1-buthyl-3-methylpyridinium chloride) to pretreat the lignocelluloses. An important result in this regard is

that acceleration in enzymatic saccharification was resulted from the decrease in the degree of polymerization (DP) of cellulose by ILs pretreatment.[18] A loose and disordered structure of bagasse resources was observed after ILs pretreatment, which contributed higher enzymatic digestibility of lignocelluloses compared to the traditional pretreatments.[19] A combined method for pretreating rice straw using ILs ([BMIM]Cl) and ammonia reagent has been recently demonstrated to increase biodigestibility of lignocelluloses and also the reutilization of IL for cost minimization.[20] The use of commercial IL of [BMIM]Cl (1-butyl-3-methylimidazolium chloride salt) have some drawbacks,[20–22] including high viscosity and slow fluidity at lower temperatures; thus, a carrier should be designed to aid [BMIM]Cl into the inner structure of lignocelluloses. Microemulsion is considered as a suitable system for [BMIM]Cl because it has a nanoscale diameter, favorable fluidity, lower surface tension, dispersible uniformity, wide electrochemical window, and favorable thermostability.[23–25] To maintain the physical actions between [BMIM]Cl and lignocelluloses, any moisture is prevented from mixing process in the system.[26,27] In this work, [BMIM]Cl and [BMIM]PF_6, were selected as aqueous and oil phases of microemulsion, respectively, to reduce the amount of unrecyclable chemicals. A suitable amount of emulgators (CTAB and *n*-butyl alcohol) was added to obtain a novel anhydrous IL microemulsion. In this system, the pretreatment of [BMIM]Cl influences the structure of lignocelluloses. [BMIM]Cl and [BMIM]PF_6 can be separated from *n*-butyl alcohol by vacuum distillation. Thus, this new microemulsion combining ILs with different characteristics can be used as a more suitable system for pretreatment of lignocelluloses.

In this article, the conductivity, surface tension of the designed anhydrous IL microemulsion system was investigated, and pseudo ternary phase diagram was established. The experiment of saccharification was carried out for the pretreated lignocelluloses (Masson Pine Powder).

EXPERIMENTAL

Materials

The following chemicals/reagents were used in the study: masson pine powder (diameter > 250 μm); CTAB (analytically pure); *n*-butyl alcohol (analytically pure); [BMIM]Cl (purity 99%); [BMIM]PH_6 (purity 99%); deionized water; and quadrol solution (volume ratio of quadrol solution to deionized water = 1 : 5); cellulase(Sigma C1184, enzymatic activity: 1300 μ/g), citric acid–sodium citrate buffer solution (pH=4.8).

Instruments

The following instruments were used: heating magnetic stirrer (DF-101S); conductivity meter (DDSJ-308A); thermogravimetric analysis (TG) (Q500TGA); X-ray diffraction (XRD) (D8 ADVANCE); scanning electron microscope (SEM) (S-3700); electronic balance (HANGPING FA2004); surface contact angle measurement instrument (OCA40 MICRO); and Fourier-transform infrared (FT-IR) (VECTOR33); ion chromatograph (Dionex ICS3000).

Conductivity

A specific conductivity meter (DDSJ-308A) was used and calibrated with KCl. The repeatability and the accuracy of this instrument were ±0.3 μs/cm and ±1%, respectively. The conductivity electrode and the mode of conductivity were set at 0.999. Both conductivity and temperature electrodes were inserted at the same time. Conductivity was determined after the reading showed a constant value.

Pseudo Ternary Phase Diagram

1. The initial system comprised CTAB (0.06 g), [BMIM]Cl (5 g), *n*-butyl alcohol (1.08 g), and [BMIM]PF_6 0.5 g (mass ratio of CTAB : *n*-butyl alcohol = 1/18). These substances were mixed in a reaction vessel and stirred for 20 min at 50°C until the system became clear.
2. [BMIM]PF_6 (0.5 g) was added to the system produced in step 1 and then stirred for 30 s. The resulting mixture should become muddy. If the system remained clear, another 0.5 g of [BMIM]PF_6 should be added to the system. This procedure should be repeated until the system becomes muddy. The total mass of [BMIM]PF_6 was recorded. The emulgator was then added at a ratio of 1 : 18 (CTAB : *n*-butyl alcohol = 0.02 : 0.36 g), stirred, and observed. After the system recovered a clear mixture, the amounts of CTAB and *n*-butyl alcohol were recorded.

Process of Pretreatment

Oven-dried powder (3 g) was mixed with quadrol solution at a liquid–solid ratio of 30 : 1. The closed reaction vessel was placed in an oil bath pan, heated for 3 h at 80°C, and stirred continuously. Afterward, the powder was removed by suction filtration, washed thrice with distilled water, and dried at 105°C until the powder was completely dry. Then the dried powder was mixed in anhydrous IL microemulsion (mass ratio of CTAB : *n*-butyl alcohol : [BMIM]Cl : [BMIM]PF_6 = 1 : 18 : 24 : 8) at a liquid–solid ratio of 30 : 1. The mixture was then heated in an oil bath pan for 8 h at 80°C. The vessel was removed and 40 mL of distilled water was added to terminate the actions after the solution was stirred for 10 min. The powder was washed with distilled water thrice, collected, and allowed to dry completely.

FT-IR Analysis

The chemical structures of products: masson pine powder and the pretreated samples were performed on a VECTOR33 FTIR spectrophotometer using a standard KBr pellet technique. Each spectrum was recorded with 25 scans in the frequency range 4000–400 cm^{-1} with a resolution of 4 cm^{-1}.

XRD Analysis

The crystal structures of Masson pine powder and the pretreated samples were investigated using an XRD analyzer (D8 ADVANCE X-ray diffractometer) set at 40 kV and 30 mA. Wide-angle X-ray intensities were collected for 2θ, ranging from 5° to 50°, with a step increment of 0.02°. The degree of crystallinity is calculated by the following equation[28]:

$$\mathrm{CrI}(\%) = 100 \times [(I_{002} - I_{\mathrm{am}})/I_{002}] \quad (1)$$

where CrI is the crystalline index, I_{002} is the maximum intensity of the 002 lattice diffraction, near $2\theta = 22.6°$, and I_{am} is the

Table I. Initial System Components in Figure1

Sample	A	B	C	D
CTAB (g)	1	1	1	0
n-Butyl alcohol (g)	12	12	0	12
[BMIM]Cl (g)	10	0	10	10
[BMIM] PF_6 (g)	0	4	4	4

intensity diffraction at suitable locations for the amorphous background at $2\theta = 16.2°$.

TG Analysis

TG analysis (TGA) was carried out for studying the thermal stability of the Masson pine powder and the pretreated samples. A TGA Q500 instrument was used to record weight loss within the range of room temperature to 700°C, with a heating rate of 10°C/min. The flow rate of nitrogen is 30 mL/min.

Scanning Electron Microscopy Analysis

A SEM was used to examine the surface image of the Masson pine powder and the pretreated samples. The samples were fixed to a metal-base specimen holder using double-sided, sticky tape. The fixed samples were coated with approximately 30 Å of Au/Pd, and were then observed using a S-3700 SEM.

Enzymatic Hydrolysis

Batch enzymatic saccharification of the Masson pine powder and the pretreated samples were carried out at 50°C in a reciprocating shaker for 24 h with 120 rpm. The liquid–solid ratio was 30 : 1, and diluted with sodium citrate buffer to a pH of 4.8. The powder samples were bone dry and the dosage of cellulase (sigma C-1184) was 100 μ/g. The yield of glucose in supernatant was measured by ion chromatograph analysis after proceeding centrifugation at 10,000 r/min for 10 min.

Ion Chromatograph Analysis

Glucose supernatant was diluted to 1—10 ppm with deionized water, 1.5 mL diluted supernatant was transferred into vial in Ion Chromatograph measurement (Dionex ICS3000,ANASTAR company, US). Analytical column and guard column were CarboPac PA1 2 × 250 mm and CarboPac PA1 2 × 50 mm, respectively. NaOH of 0.001 mol and 0.05 mol Na_2AC were used as the leacheate. Volume flowrate was 0.650 mL/min, injection volume was 10 μL and temperature was 30°C.

RESULTS AND DISCUSSION

Conductivity

Conductivity analysis is an important method used to monitor the change in state of microemulsion continuously, obtain useful information of dynamic processes, and ensure the type of structure and stability of microemulsion.[29]

Table I lists the initial system components. A higher conductivity level should be maintained to retain the combination between Cl^- of [BMIM]Cl and H^+ of the hydrogen bond in a biomass. Figure 1 shows that [BMIM]PF_6 slightly contributed to conductivity. For this reason, we did not discuss this phenomenon in this study. The other components have important functions to enhance conductivity. In particular, the viscosity of

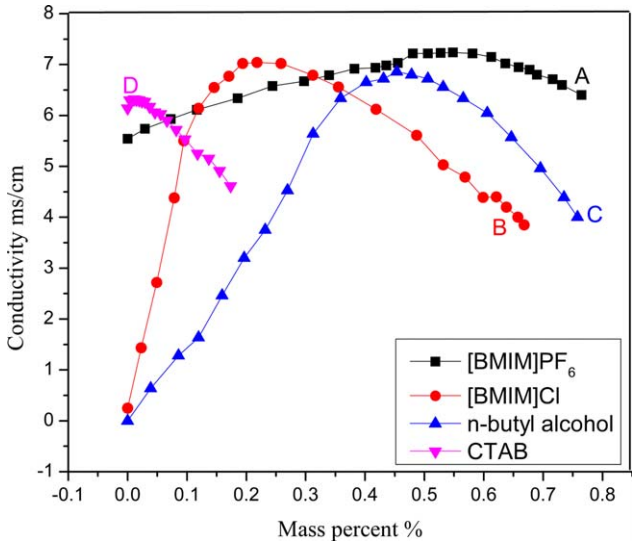

Figure 1. Effect of the dosage of each component on the conductivity of microemulsion. [Color figure can be viewed in the online issue, which is available at wileyonlinelibrary.com.]

the system decreased after higher amounts of *n*-butyl alcohol were added as a co-surfactant and solvent. Thus, the resistance to motion of Cl^- decreased, but conductivity increased. By contrast, conductivity decreased when excessive amounts of *n*-butyl alcohol were present because the system became diluted. As [BMIM]Cl content increased, Cl^- content and conductivity increased simultaneously, but excessive [BMIM]Cl increased viscosity. This increase in viscosity prevented the ion to move freely. As a result, conductivity decreased evidently. The effect of conductivity from CTAB depended on its ability to form a composite membrane with *n*-butyl alcohol. At lower amounts of CTAB, an effective monolayer interfacial film was formed with *n*-butyl alcohol to produce higher conductivity. Likewise, an excess amount of CTAB formed a very thick interfacial film with surplus products, which are harmful for the formation of a clear system. Conductivity then decreased rapidly. Considering that lower amounts of CTAB have an important effect on conductivity, the amount should be further investigated.

Table II lists the initial system components. Figure 2 shows the curve with a characteristic initial increase; after a peak value was reached, the curve showed a decreasing trend. Figure 2 further shows that the conductivity of the system reached the maximum value with 0.25 g of CTAB, but other conditions remained constant. At the same time, the change in conductivity was homogeneous. At 0.5 g of CTAB, the curve satisfied the demand of high conductivity and homogeneous change similarly. In contrast to the two aforementioned curves, the other

Table II. Initial System Components in Figure 2

Sample	A	B	C	D	E
CTAB (g)	1	0.75	0.5	0.25	0.1
[BMIM]Cl (g)	5				
n-Butyl alcohol (g)	6				

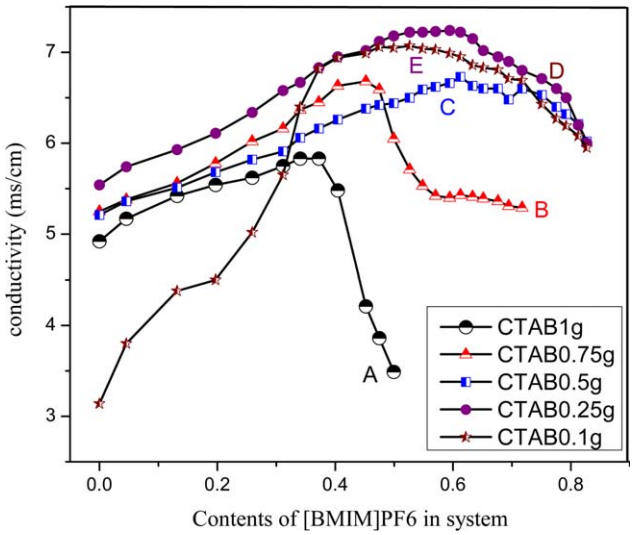

Figure 2. Effect of different dosage of CTAB on the conductivity of microemulsion. [Color figure can be viewed in the online issue, which is available at wileyonlinelibrary.com.]

curves showed heterogeneous changes. Such changes prevented the formation of a stable system. For 6 g of *n*-butyl alcohol and 0.25 g of CTAB, the ratio of surfactant/co-surfactant was 1/24. For 6 g of *n*-butyl alcohol and 0.5 g of CTAB, this ratio was 1/12. To maintain a high conductivity level, the ratio of surfactant/co-surfactant should range from 1/12 to 1/24. In further experiments, 1/18 was selected as the most suitable value under the condition of Table II.

Pseudo-Ternary Phase Diagram

The difference in the composition proportion between microemulsion and turbid liquid can be presented in a pseudo-ternary phase diagram intuitively. A cloud point curve should be determined to confirm the standard, which should be used in further experiments that require microemulsion preparation.[30] In the study, the red star curve in the pseudo-ternary phase diagram is the same as the black curve in the right graph. A, B, and C areas correspond to one another. The [BMIM]PH_6/[BMIM]Cl region, bicontinuous region, and [BMIM]Cl/[BMIM]PH_6 region in the pseudo-ternary phase diagram also correspond to O/W, bicontinuous, and W/O in the traditional microemulsion, respectively. The folded line in the phase diagram indicates the cloud point curve, in which the system becomes turbid after the red star line crosses the curve. The microemulsion system becomes invalid thereafter. For Figure 3 The microemulsion region, or the transparent region, occupies >75% of the area in the phase diagram (Figure 3). A clear system is difficult to obtain when the amounts of [BMIM]Cl and [BMIM]PF_6 are >80%. Mass ratio of CTAB : n-butyl alcohol(emulgator) = 1/18. Thus, we used a dashed line to replace the solid line to show uncertainty.

Surface Tension Analysis

Surface tension of a liquid refers to the force acting on a liquid surface to reduce the superficial area. Surface tension is an important factor that characterizes liquid properties. In this paper, surface tension was analyzed based on the hanging-drop

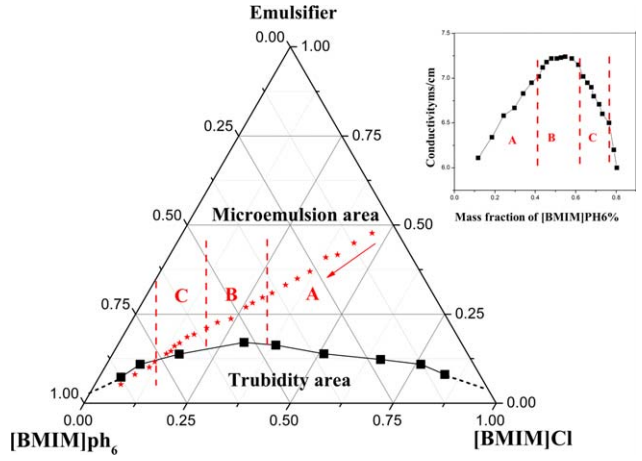

Figure 3. Pseudo-ternary phase diagram at 50°C. [Color figure can be viewed in the online issue, which is available at wileyonlinelibrary.com.]

method. The principle of this method is expressed according to Laplace's equation in terms of capillarity[31]:

$$\Delta P = \gamma\,(1/R1 + 1/R2) \qquad (2)$$

where γ is the surface tension; $R1$ and $R2$ are the radii of the curved surfaces; and ΔP is the pressure difference on the surface.

Table III shows the system components. The averages of surface tension in experiments A and B were 25.1 and 25.5 mN/m in Figure 4, respectively. These averages were both less than the surface tension of water (72.75 mN/m), which is commonly used as a solvent. Table III shows that the amount of [BMIM]Cl in A was twice the amount added to the system in B, and such an amount of [BMIM]Cl easily surrounds [BMIM]PF_6 to form a [BMIM]PF_6]/[BMIM]Cl microemulsion. Thus, the fluidity in A is more efficient than that in B. This observation of the smaller surface tension of A than B can also be explained according to the following. At constant temperature and amounts of surfactant and co-surfactant, more organic solvents can have lower surface tension.[23] IL is also called an organic IL;[25] thus, the surface tension in experiment A should be lower than that in experiment B. Although the results slightly differed, the surface tension in these two experiments ranged from 24.5 to 25.5 mN/m that corresponds to the surface tension of traditional microemulsion.[11,28,30]

Microscopic Particle System of IL Microemulsion

The types of microemulsion include aqueous phase/oil phase, bicontinuous, and oil phase/aqueous phase. Given that hydrophilic [BMIM]Cl is the main reagent that reacts with powder, hydrophilic [BMIM]Cl was selected as the main composition and continuous phase to prepare oil phase/aqueous phase of IL

Table III. System Components of Experiment A and B in Figure4

	CTAB (g)	*n*-Butyl alcohol (g)	[BMIM]Cl (g)	[BMIM]PF_6 (g)
A	0. 5	9	12	4
B	0. 5	9	6	4

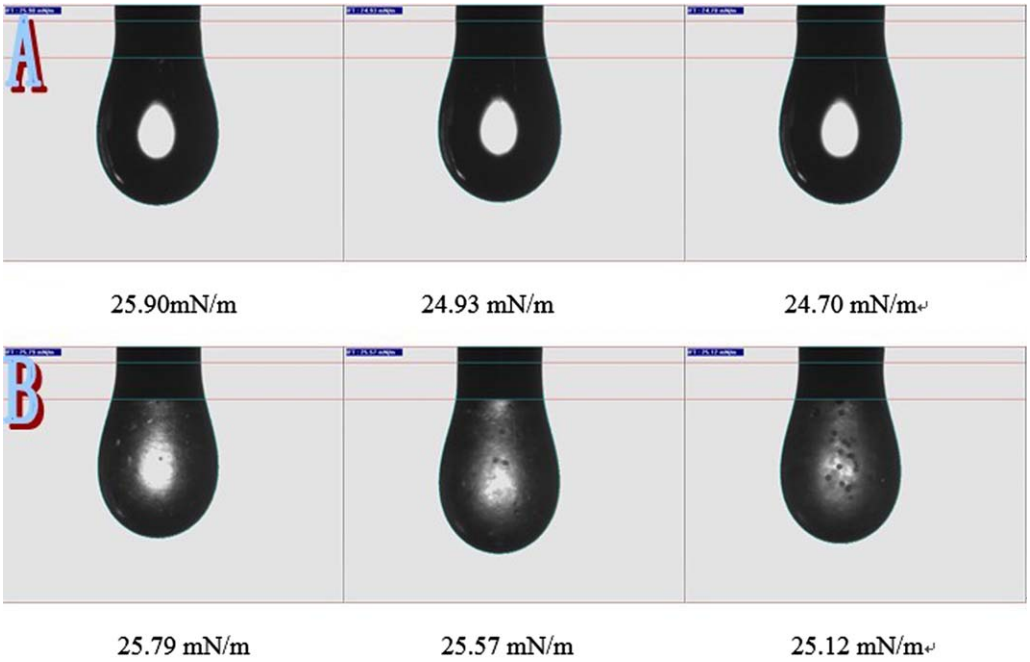

Figure 4. Surface tension of IL microemulsion. [Color figure can be viewed in the online issue, which is available at wileyonlinelibrary.com.]

microemulsion in this article. Figure 5 shows the microscopic particle system, in which the dispersion phase [BMIM]PF_6 is the core and the emulgators (CTAB and *n*-butyl alcohol) comprise the monolayer-mixed film with a mosaic structure. The hydrophobic tail of CTAB is oriented toward the core, whereas the hydrophilic head is projected outside the film and bound to a dissociated Cl^- from [BMIM]Cl by principle of similarity and intermiscibility. The microscopic system of [BMIM]PF_6/[BMIM]Cl can only be established in this manner.

IR Analysis

FT-IR spectroscopic analysis is performed to determine structural changes in cellulose or lignocellulosic biomass after these substances are subjected to pretreatments. The combined pretreatments have a synergistic effect—quadrol treatment broke

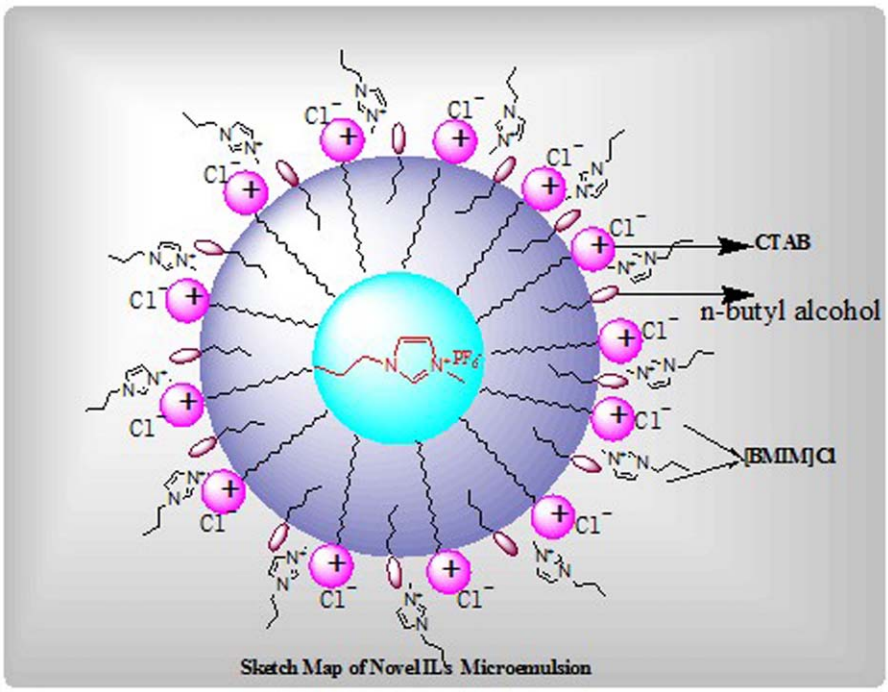

Figure 5. Microscopic particle system of IL microemulsion. [Color figure can be viewed in the online issue, which is available at wileyonlinelibrary.com.]

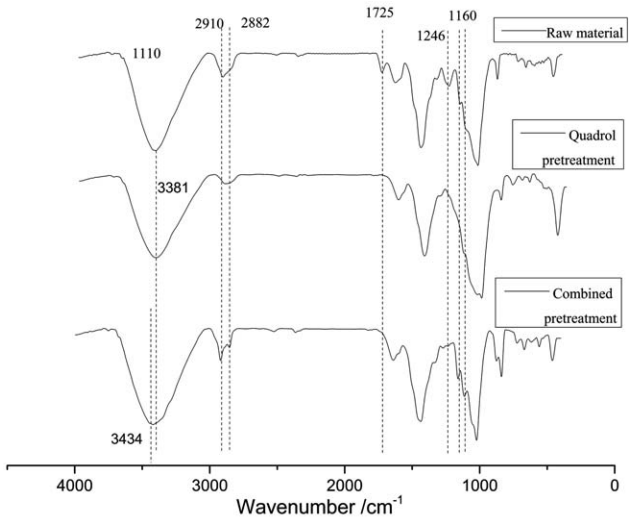

Figure 6. FT-IR analysis of powder before and after pretreatment.

the structure of hemicellulose and ILs microemulsion treatment broke the net structure of hydrogen bond in noncrystalline region of cellulose, partly, both of them are helpful for a loose and multihole structure. We analyzed the biomasses before and after pretreatment at a range of 400–3600 cm^{-1}.[18]

The solubility of cellulose can be increased by destroying or weakening the hydrogen bonds present in cellulose.[32] Intramolecular hydrogen bonds are formed between O(2)H…O(6) and O(3)H…O(5) of cellulose and can be identified by the presence of bands at wavenumbers of 3455 −3410 cm^{-1} and 3385–3340 cm^{-1}, respectively.[31] Peak shifts can be observed in Figure 6 in the region with a high wavenumber from 3381 to 3434 cm^{-1} after combined pretreatment, indicating that the network of hydrogen bonds is altered in the cellulose structure.

The characteristic peaks of cellulose are 2900, 1425, and 1374 cm^{-1}. The stretching vibration of C=O on acetyl and carboxyl as well as the absorption peak of ether linkage are both 1725 cm^{-1}, which is the characteristic peak of hemicellulose and the bond between LCC (connection bond between lignin and hemicellulose). This peak disappeared after pretreatment, indicating that a partial amount of hemicellulose underwent deacetylation to produce organic acids and thus caused the bond between LCC to break.[33] Considering the three lines, deacetylation occurred during quadrol pretreatment. The absorption peaks of lignin and hemicellulose are both 1246 cm^{-1}. The disappearance of this peak also contributes to the increase in relative crystallinity.

The powder was pretreated with IL microemulsion based on quadrol pretreatment. This procedure caused the peak at 2900 cm^{-1} to split in two peaks (2882 and 2910 cm^{-1}), indicating that a part of the crystalline region of cellulose I is broken and recrystallized to form cellulose II. The stretching vibration of C–O–C and the corresponding band of O–H are seen at 1160 and 1110 cm^{-1}, respectively. These values are the common characteristic peaks of cellulose and hemicellulose. The quadrol pretreatment did not change the strength of the peaks at 1160 and 1110 cm^{-1}, but these two peaks increased after IL microemulsion pretreatment was performed. The change in these two peaks indicated that free hydrogen bond increased after IL microemulsion pretreatment was conducted. The disappearance of the peak at 1725 cm^{-1} indicated that hemicellulose was largely removed. Thus, the change in peak at 1160 and 1110 cm^{-1} resulted from the breakage and restructuring of hydrogen bonds from less amounts of hemicellulose and large noncrystalline region of cellulose; as a result, relative crystallinity increases.[11] Higher amounts of exposed cellulose are helpful for saccharification. To understand the crystalline structure, XRD measurements of the pretreated biomass were conducted.

Crystal Structure Analysis

Crystallinity has been proven as a significant factor affecting the enzymatic saccharification of cellulose.[26,36] Different pretreatments can change cellulose crystal structures by disrupting inter- and intrachain hydrogen bonding of cellulose fibrils.[1] Two primary peaks are formed in untreated and treated biomass. The first peak was broad measuring approximately 16°. The second peak appeared at 22.5°. Equation (2) shows that I_{002} is the intensity of the crystalline portion of biomass (cellulose I) and I_{am} is the peak of the amorphous portion (cellulose, hemicelluloses, and lignin).[37] Before any pretreatment, the relative crystallinity index of the powder is 35.8. After quadrol treatment was performed, a part of hemicellulose structure was broken and removed by quadrol, so the relative proportion of noncrystalline region reduced, and this proportion of crystalline region increased. Thus, this relative crystallinity index was effectively increased to 41.5. In the case of the following IL microemulsion treatment, crystallinity was increased to 49.8 and this step of pretreatment caused the I_{002} peaks to split in two peaks (20° and 22°). These characteristics are quite similar to the diffraction pattern of cellulose II as previously reported.[38] After the combined pretreatment (quadrol+ILs microemulsion), the relative crystallinity index increased by 39%. This increase resulted from the removal of hemicellulose and noncrystalline region of cellulose; a part of cellulose I was recrystallized, forming cellulose II.[34] Cellulose became more exposed; an increase in cellulose surface accessibility is observed and theoretically enables a more efficient cellulose hydrolysis to occur.[1]

Thermogravimetric Analysis-Derivative Thermogravimetry Analysis

The main pyrolysis region of lignocellulosic biomass ranges from 150°C to 450°C. Hemicellulose, which is polymerized with different sugar units, is the easiest part to undergo pyrolytic reaction among the three major components of biomass. Hemicellulose is found in an amorphous region ranging from 190°C to 335°C. More hemicelluloses reveal a more evident peak at this low-temperature region. For cellulose, the main pyrolysis region ranges from 260°C to 395°C. Lignin has an amorphous straight-chain polymer, which has a networked structure containing pyrolytic chemical components that can be broken either easily or difficultly; thus, the pyrolytic region sufficiently ranges from 200°C to 700°C[39] The major carbonization processes occur in the region with temperatures > 450°C, in which residues such as ash and coke are resistant to high temperatures.

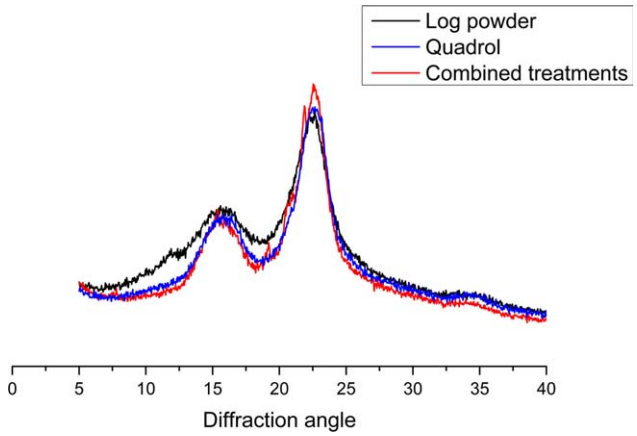

Figure 7. XRD analysis before and after pretreatment. [Color figure can be viewed in the online issue, which is available at wileyonlinelibrary.com.]

Figure 8(A) shows that the beginning of the region where the main thermal weight loss occurred remains unchanged, whereas the end of this region shifted from 375°C to a low temperature zone at 310°C after the two-step pretreatment. As a result, the main part of the pyrolytic region shortened to a lower temperature range, indicating that thermostability decreased. This decrease occurred because hydrogen and chemical bonds on hemicellulose and noncrystalline region of cellulose were disrupted. The decreased strength between fibers is the original factor that causes lignocellulosic materials to undergo pyrolysis easily.

Figure 8(B) shows that the powder has two main thermal weight loss peaks at 318°C and 375°C before any pretreatment. In cellulose degradation, the region at a peak of 318°C is the area where rapid degradation of hemicellulose occurs. The highest thermal weight loss peak at around 375°C is the region where cellulose degradation occurs. This peak shifted to a low-temperature region and split in two peaks (285°C and 310°C). The peaks at 310°C and 285°C are the main weight loss peaks of cellulose I and cellulose II, respectively. The peak of cellulose II is weaker than that of cellulose I, because cellulose II has fewer contents. This phenomenon is consistent with the result shown in Figures 6 and 7.[10] The peak of hemicellulose disappeared after the treatment, indicating that a large amount of hemicellulose was removed. The breakage and recombination of the chemical structure in biomass can contribute to lower temperature of the main pyrolytic region, faster rate of degradation, and weak stability of biomass. These factors contribute to permeation and actions with cellulose, thereby obtaining a higher efficiency of saccharification.

SEM Analysis

SEM can provide a more visualized image to understand the change in microstructure before and after pretreatment. Before any treatment, the microscopic surface texture of the powder is smooth without a cover, the bottom of the pit is closed, and the main structure is compact. This structure functions as a barrier preventing chemicals to enter the interior structure of

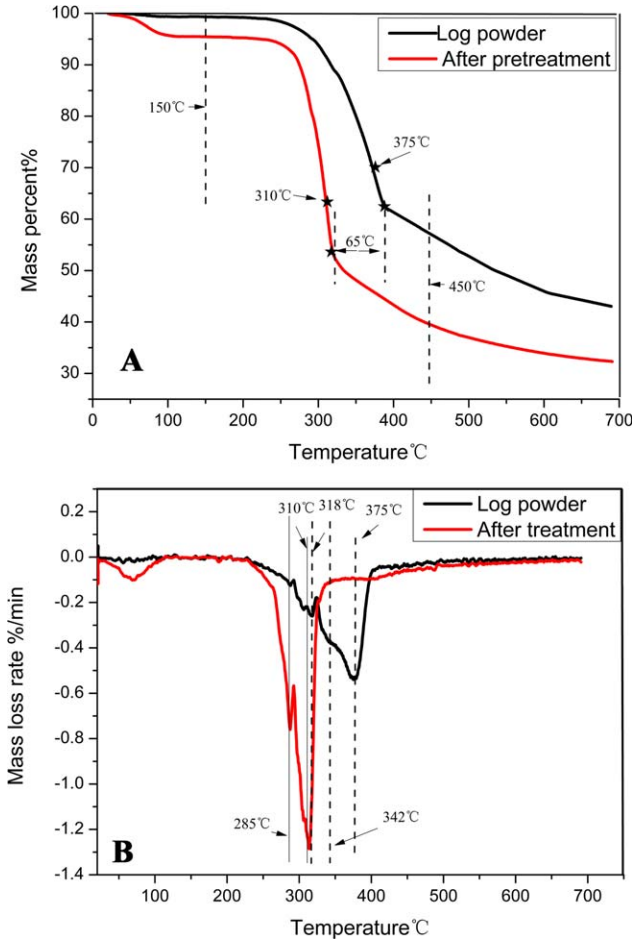

Figure 8. Thermogravimetric analysis-Derivative Thermogravimetry analysis before and after combined pretreatment. [Color figure can be viewed in the online issue, which is available at wileyonlinelibrary.com.]

the biomass. After pretreatments, especially the combined pretreatment, the cover on the microscopic surface and roughness increased. The bottom of the pit was broken, thereby opening the passageway. The specific surface area and accessibility were increased. So the decrease in structural compactness could promote the efficiency of saccharification. We have no detailed data, we just can understand the change of hole and surface structure of powder, intuitively (Figure 9).

Enzymatic Hydrolysis

The enzymatic hydrolysis of the masson pine powder was comparatively investigated using the method of quadrol, anhydrous IL microemulsion, and the combined method, respectively. Hydrolysis conditions were discussed as follows: liquid–solid ratio 30 : 1, pH4.8, 50°C 24 h 100 μ/g (sigma). The results showed that the glucose yield of the masson pine powder and the treated samples using quadrol, anhydrous IL microemulsion, and the combined method were 35.8%, 56.1%, 67.3%, and 78.2%, respectively. These data proved that combined pretreatment really have the satisfied effect to increase the glucose yield of lignocellulose. The observations between the different glucose yields demonstrated the large influence of pretreatment of the anhydrous IL microemulsion on efficiency of enzymatic hydrolysis for lignocellulose.

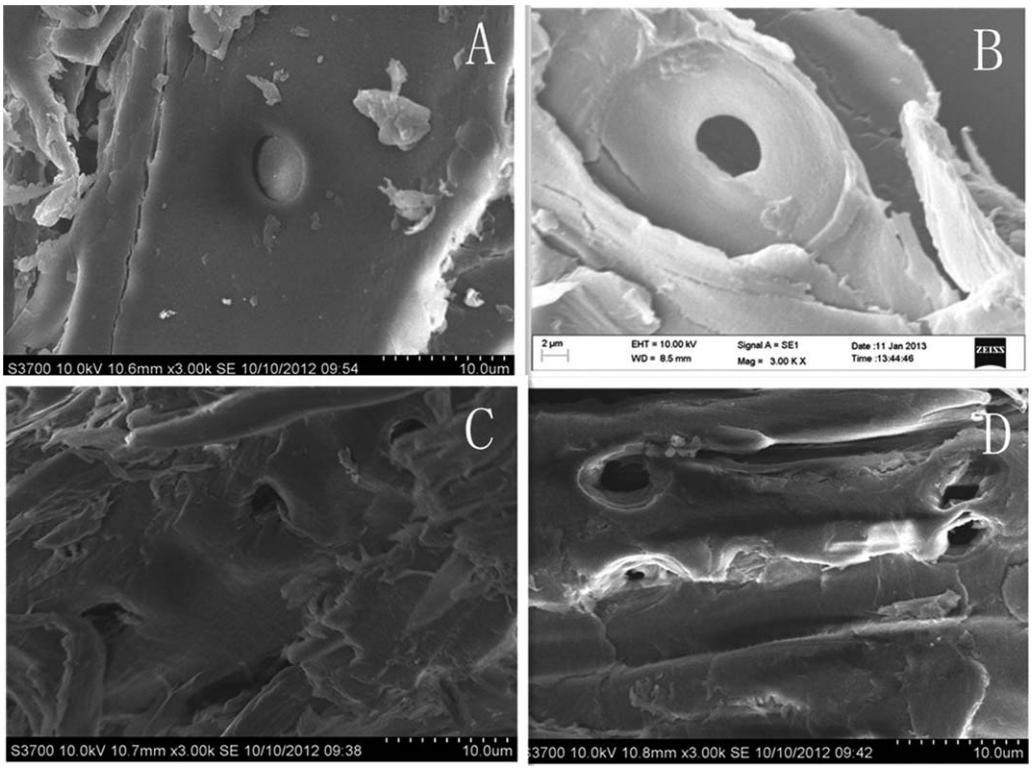

Figure 9. SEM of the powder before and after pretreatment. (A) Before pretreatment. (B) After quadrol pretreatment. (C) After ILs microemulsion pretreatment. (D) After combined pretreatment.

CONCLUSION

1. We selected [BMIM]Cl and [BMIM]PF_6 as aqueous and oil phases, respectively, to eliminate water in the system. The effective function between Cl^- and hydrogen bond on cellulose and hemicellulose can be maintained in this way. High conductivity indicates the suitable concentration and flowability of Cl^-. To increase the amount of [BMIM]Cl, we need to limit the ratio of surfactant/co-surfactant in the range of 1/24 to 1/12. Microemulsion system overcomes the defects caused by high viscosity and low flowability of [BMIM]Cl.
2. IR and XRD reveal that the characteristic peaks of hemicellulose (1246 cm^{-1} and 1725 cm^{-1}) disappear and the relative crystallinity increases from 35.8 to 49.8. This result indicates that hemicellulose and the noncrystalline region of cellulose are broken and eliminated effectively. TG indicates that the thermostability of the powder decreased. The major part of the pyrolysis region shifts from 375°C to a low-temperature zone at 310°C. The degradation rate speeds up, indicating that hydrogen and chemical bonds are disrupted effectively. IR, XRD, and DTG show that a few crystalline regions of cellulose are recrystallized to form cellulose II. The variation occurs at 2920 cm^{-1} (IR), 22.6 (XRD), and 285–310°C (DTG). These results show that the combined pretreatment is an effective method used to change the physicochemical property of masson pine. In particular, a loose and highly accessible structure make the glucose yield increased from 35.8% to 78.2% after combined pretreatment, which is a satisfied result for fermentation process, further.

ACKNOWLEDGMENTS

This study is financially supported by the National Key Technology R&D Program (Grant No. 2013BAC01B03), the National Natural Science Foundation of China (Grant No. 31000285), the Key Scientific and Technological Project in Guangdong Province (Grant No. 2012A010800026), and the Special Insulating Paper School-Enterprise Cooperation Innovation Laboratory Construction Project of South China University of Science and Technology (Grant No. Y1110090).

REFERENCES

1. Li, C.; Knierim, B.; Manisseri, C.; Arora, R.; Scheller, H. V.; Auer, M.; Vogel, K. P.; Simmons, B. A.; Singh, S. *Bioresour. Technol.* **2010**, *101*, 4900.
2. Jung, Y. H.; Cho, H. J.; Lee, J. S.; Noh, E. W.; Park, O. K. and Kim, K. H. *Bioresour. Technol.* **2013**, *129*,639.
3. Simmons, B. A.; Loque, d.; Blance, H. W. *Genome Biol.* **2008**, *9*, 242.
4. Zhu, J. Y.; Pan, X. *J. Bioresour. Technol.* **2010**, *101*, 4992.
5. Yoshida, M.; Liu, Y.; Uchida, S.; Kawarada, K.; Ukagami, Y.; Ichinose, H.; Kaneko, S.; Fukuda, K. *Biosci. Biotechnol. Biochem.* **2008**, *72*, 805.
6. Weerachanchai, P.; Leong, S. S. J.; Chang, M. W.; Ching, C. B.; Lee, J. M. *Bioresour. Technol.* **2012**, *111*, 453.
7. Uju Nakamoto, A.; Shoda, Y.; Goto, M.; Tokuhara, W.; Noritake, Y.; Katahira, S.; Ishida, N.; Ogino, C.; Kamiya, N. *Bioresour. Technol.* **2012**, *6*, 96.

8. Wei, W. Q.; Wu, S. B.; Liu, L. G. *Bioresour. Technol.* **2013**, *128*, 728.
9. Percival, Y. H.; Eric, Z.; Simo, B.; Bruce, S.; Dale, E. *Appl. Biochem. Biotechnol.* **2009**, *153*, 80.
10. Pejo, E. T.; Oliva, J. M.; Ballesteros, M. *J. Sci. Ind. Res.* **2008**, *67*, 874.
11. Wang, B. Application of Ironic Liquid Microemulsion Pretreatment Process in Biomass Conversion. Master thesis, South China University of Technology, Rendang Yang, June **2012**.
12. Zheng, Y.; Pan, Z. L.; Zhang, R. H. *Int. J. Agric. Biol. Eng.* **2009**, *2*, 51.
13. Keshwani, D. R.; Cheng, J. J. *Bioresour. Technol.* **2009**, *100*, 1515.
14. Lloyd, T. A.; Wyman, C. E. *Bioresour. Technol.* **2005**, *96*, 1967.
15. Njoku, S. I.; Ahring, B. K.; Uellendahl, H. *Bioresour. Technol.* **2012**, *124*, 105.
16. Balat, M. *Bioresour. Technol.* **2011**, *52*, 858.
17. Ren, H. F.; Zhou, Y. G.; Liu, L. *Bioresour. Technol.* **2013**, *129*, 616.
18. Uju Shoda, Y.; Nakamoto, A.; Masahiro, G.; Tokuhara, W.; Noritake, Y.; Katahira, S.; Ishida, N.; Nakashima, K.; Ogino, C.; Kamiya, N. *Bioresour. Technol.* **2012**, *103*, 446.
19. Qiu, Z. H.; Aita, G. M.; Walker, M. S. *Bioresour. Technol.* **2012**, *117*, 251.
20. Nguyen, T. A. D.; Kim, K. R.; Han, S. J.; Cho, H. Y.; Kim, J. W.; Park, S. M.; Park, J. C.; Sim, S. *J. Bioresour. Technol.* **2010**, *101*, 7432.
21. Wang, B.; Yang, R. D.; Shi, W. J.; Liu, D. T.; Zhu, L. *Acta Chim. Sinica.* **2011**, *69*, 3013.
22. Long, J. X.; Guo, B.; Li, X. H.; Jiang, Y. B.; Wang, F. R.; Tsang, S. C.; Wang, L. F.; Yu, K. M. K. *Green Chem.* **2011**, *13*, 2334.
23. Wang, J.; Yang, X. Z. Preparation and application of microemulsion; China Textile Press: Beijing, **2011**; Vol. *2*, Chapter 3, p 24.
24. Zhuang, Y. Q.; Ke, X.; Zhan, X. L.; Luo, Z. H. *Powder Technol.* **2010**, *201*, 146.
25. Tian, Q. P.; Ren, F. D.; Xu, Z.; Xie, Y.; Zhang, S. Q. *Int. J. Pharm.* **2012**, *426*, 202.
26. Zhang, X. C. Ionic Liquid. Chemical Industry Press: Beijing, **2009**; Vol. *3*, Chapter 12, p234.
27. Dadi, A. P.; Schall, C. A.; Varansi, S. *Appl. Biochem. Biotechnol.* **2007**, *136*,407.
28. Cheng, S. Q.; Fu, X. G.; Liu, J. H.; Zhang, J. J.; Zhang, Z. F.; Wei, Y. L.; Han, B. X. *Colloids Surf. A.* **2007**, *302*, 211.
29. Mehta, S. K.; Kaur, G.; Mutneja, R.; Bhasin, K. K. *J. Colloid Interface Sci.* **2009**, *338*, 542.
30. Ma, J. J.; Wu, B. *Adv. Powder Technol.* **2013**, *24*, 354.
31. Xi, X. G.; Chen, P. *J. Yancheng Inst. Technol. Natural Sci. Ed.* **2008**, *21*, 1.
32. Xu, A.; Wang, J. J.; Wang, H. Y. *Green Chem.* **2009**,*12*, 268.
33. Zhang, X. Y.; Zhao, G. J. *J. Beijing Forestry Univ.* **2008**, *30*, 101.
34. Wang, K. Research on Pretreatment, Component Fractionation and Enzymatic Hydrolysis of Lignocellulosic Materials. Ph.D. thesis, Beijing: Beijing Forestry University, Runcang Sun, June **2011**.
35. Dadi, A. P.; Varanasi, S.; Schall, C. A. *Biotechnol. Bioeng.* **2006**, *95*, 904.
36. Kumar, R.; Mago, G.; Balan, V.; Wyman, C. E. *Bioresour. Technol.* **2009**, *100*, 3948.
37. Cheng, G.; Varanasi, P.; Li, C. L.; Liu, H. B.; Melnichenko, Y. B.; Simmons, B. A.; Kent, M. S.; Singh, S. *Biomacromolecules* **2011**, *10*,1012.
38. Isogai, T.; Yanagisawa, M.; Isogai, A. *Cellulose* **2009**, *16*, 117.
39. Yang, H. P.; Yan, R.; Chin, T.; Liang, D. T.; Chen, H. P.; Zheng, C. G. *Energy Fuels* **2004**, *18*, 1814.